

THE EFFECTIVE ATOMIC NUMBERS AND THE EFFECTIVE ELECTRON NUMBERS OF SOME STEELS AT DIFFERENT GAMMA ENERGIES

Elif Maril,

Department of Property Protection and Security,
Yenice Vocation School, Karabük University, 78050, Karabuk, Turkey
Corresponding Author, elifmaril@karabuk.edu.tr

Hasan Gumuş

Ondokuz Mayıs University, Science and Arts Faculty,
Physics Department, 55 139, Samsun, Turkey
hgumus@omu.edu.tr

ABSTRACT

In this study, the effective atomic numbers (Z_{eff}), the effective electron number (N_{eff}), the half value layer (HVL) and the mean free path (λ) for two different steels have been determined at Co-60 and Eu-152 energies. The measurement of linear attenuation coefficients at 122, 245, 344, 444, 779, 867, 964, 1112, 1173, 1333 and 1408 keV energies was made using a gamma spectrometer system with a NaI (TI) detector connected to Multi-Channel-Analyzer (MCA). The experimental half value thickness and the mean free path were found to be in good agreement with the calculation results. Also, effective atomic numbers (Z_{eff}) and effective electron number (N_{eff}) parameters were calculated using the EpiXS 2021 and the results were evaluated.

Keywords- The cross sections, effective atomic numbers, stainless steels, half value layer, mean free path.

1. INTRODUCTION

With increasing energy demand and advancement in technology, the use of radiations is increasing rapidly in our daily lives. The use and applications of γ rays are increasing rapidly in various fields such as nuclear and radiation physics, industry, medicine, power generation and agriculture [1]. In addition to the many great advantages and benefits that nuclear technology provides to humanity, there are also some disadvantages associated with radiation. γ radiation and high energetic x-rays are used in radiotherapy for cancer treatment in order to destroy unhealthy tissues along with the cancer cells in human body [2,3]. The photon mass attenuation coefficient, Z_{eff} , and the N_{eff} are the fundamental quantities in determining the penetration of X and γ -ray in matter [4, 5, 6, 7].

These highly penetrating and high energy ionizing radiations are harmful to the human body, sensitive laboratory equipment, animals, and environment. Therefore, it is important to study γ radiation in applied radiation fields, medical physics involving radiation for therapeutic and diagnostic use, radiation physics, reactors shielding etc. [2, 3, 8,9]. The study of highly penetrating gamma photons and interactions of highly energetic photons with different type of materials is also of prime importance in basic physics.

The carbon steel and stainless alloys are the common structural materials of nuclear reactors for calandria shell, end shield for primary heat transport system and moderator system [10,11]. Due to the development of nuclear technology over time, various beneficial applications of different types of radiations in medicine, industry, agriculture, and research as well as for nuclear energy production are increasing day by day. However, a disadvantage of these peaceful uses of radiation is that a harmful effect can be observed if the radiation is exposed to the personnel including other people nearby, beyond the allowable dose limit. When radiation is exposed to tissues or organs, it loses some its energy through different kinds of interactions and

this loss of energy may ionize the atoms of the cell, destroying the normal chemical equilibrium of the cell and eventually can bring death to the cell [12]. Therefore, the radiation must be attenuated enough to protect the personnel from the harmful effects caused by it also enable them to work by using an opposite shielding material. In the case of special purpose of radiation shielding lead and steel can be used as heavy weight aggregates.

The aim of this our study is to provide available information concerning using this kind of steel as a gamma shielding in nuclear applications. The well-known WinXCom program is usually employed for calculating gamma-ray and X-ray attenuation coefficient and interaction cross sections of different materials [13]. The most widely used platform for photon cross sections or mass attenuation coefficients is the XCOM [14] web program developed by NIST. Some researchers have also constructed PC-based software counterparts to XCOM, using the XCOM/NIST libraries [15, 16]. Any available computer code built on other major photon libraries that are distinct from XCOM/NIST has been scarce. An instance of such is a recent spread sheet program described in Hila et al. [17] that uses the EPICS2017 and the EPDL97 libraries to calculate mass attenuation coefficients, Z_{eff} and N_{eff} .

In this study, WinXCom program is used to calculate the partial and total mass attenuation coefficients for different compositions of Maraging steels at photon energies (1 keV-1 GeV). The mass attenuation coefficient data were then used to obtain the half value layer (HVL) and mean free path (λ) of the investigated materials and were compared with the measurements obtained at photon energies of 122, 245, 344, 444, 779, 867, 964, 1112, 1173, 1333 and 1408 keV for two different steels, namely stainless steel (S1: EN 10204) and speed steel (S2: 2367). Also the Z_{eff} and the N_{eff} of the investigated materials were obtained by using EpiXs program [18].

2 MATERIALS AND METHODS

The μ/ρ of two different types of steel, calculated using the XCOM code which uses chemical parameters of a mixture materials providing total cross sections as well as partial cross sections for various interaction processes at photon energy of 1 keV-100 GeV [15].

The detection of γ -rays was carried out using a gamma spectrometer consisting of a 10 cm diameter NaI(Tl) detector connected to the Multi-Channel-Analyzer (MCA). With the known density (ρ) of a material, the mass attenuation coefficients (μ/ρ) were obtained via measuring the linear attenuation coefficients. The theoretical μ/ρ values for the present steels were obtained by winXCcom program [19].

2.1. Linear and mass attenuation coefficient

When a gamma-ray beam passes through an absorber, the intensity of the beam will be reduced according to the Beere-Lambert's law:

$$I = I_0 \exp(-\mu x) = I_0 \exp(-\frac{\mu}{\rho} \rho x) \quad (2.1)$$

where I and I_0 are the attenuated and incident gamma ray intensities, respectively. x is the thickness of the sample in cm, μ (cm^{-1}) is the linear attenuation, ρx is are the material thickness in g/cm^2 and ρ is the material density and μ/ρ is the mass attenuation coefficient in cm^2/g [20, 21].

The half value layer HVL is the thickness of the material where one half of the incident photons is attenuated. It can be calculated via [21, 18]

$$HVL = \frac{0.693}{\mu} \quad (2.2)$$

Last parameter to be calculated is tenth value layer TVL is the thickness of the shielding material where one tenth of the incident photons is attenuated

$$TVL = \frac{2.3026}{\mu} \quad (2.3)$$

Linear attenuation coefficient is $\mu = \rho \mu_m$ and mean free path is

$$\lambda = 1/\mu \quad (2.4)$$

2.2 Effective atomic number and effective electron density

The mass attenuation coefficient for the compound or mixture can be derived from the coefficients of the component elements that are assumed to contribute to the weighted average [23, 24] (Hubbell and Seltzer, 1982, 1995):

$$\left(\frac{\mu}{\rho}\right) = \sum_i w_i (\mu/\rho)_i \quad (2.5)$$

where w_i and $(\mu/\rho)_i$ are the fractional weight and the mass attenuation coefficient of the i th constituent element, respectively. (μ/ρ) does not depend on the phase (gas, liquid, or solid) of the material. Therefore, it is useful to define the μ/ρ . This mixing rule is valid assuming that the effects of molecular binding and the chemical crystalline environment are negligible. The $\mu_m = (\mu/\rho)$ value of the alloys can be calculated for a given energy range using WinXCom software based on the mixture [19].

For a chemical compound or mixture, the fraction by weight (w_i) is given by,

$$w_i = \frac{A_i n_i}{\sum_j A_j n_j} \quad (2.6)$$

where A_i is the atomic weight of the i th element and n_i is the number of formula units and $\sum_i w_i = 1$.

Total photon interaction cross-section (σ_t) of the compound is determined with the help of the mass attenuation coefficient (μ_m) through the following equation:

$$\sigma_t = \frac{\sum A_i n_i}{N_A} \mu_m \quad (2.7)$$

A_i is the atomic weight of the i th element, n_i the number of formula units of a molecule and N_A is Avogadro's number.

The molecular cross section can be computed utilizing the above μ/ρ quantity as below

$$\sigma_{t,m} = \frac{1}{N_A} \left(\frac{\mu}{\rho}\right)_{comp} \sum (n_i A_i) \quad (2.8)$$

where N_A is the Avogadro number, n_i and A_i represent the number of element and atomic weight of the i th element in the material, respectively. The total atomic cross-section ($\sigma_{t,a}$) can be determined as follow: [25, 26, 27, 28].

$$\sigma_{t,a} = \frac{\sigma_{t,m}}{\sum n_i} \quad (2.9)$$

The total electronic cross-section ($\sigma_{t,e}$) can be expressed as follow [22]

$$\sigma_e = \frac{1}{N_A} \sum \frac{f_i A_i}{Z_i} \left(\frac{\mu}{\rho}\right)_i \quad (2.10)$$

where f_i denotes the fractional abundance of the element i and Z_i the atomic number of constituent element and $(\mu/\rho)_i$ is the total mass absorption coefficient of the element. The Z_{eff} is related to σ_a and σ_e through the following equation [4, 25, 29, 30]

$$Z_{eff} = \frac{\sigma_{t,a}}{\sigma_{t,e}} \quad (2.11)$$

The interpolation method is considered more complex to execute than the direct method because of required elemental database and the possibilities for multivalued Z_{eff} [18, 31, 32].

The effective electron density, (number of electrons per unit mass, N_{eff}) of the sample can be calculated from the relation

$$N_{eff} = \frac{Z_e N_A}{A_{comp}} \sum n_i (\text{electron/g}) \quad (2.12)$$

$$N_{eff} = Z_{eff} \frac{N_A}{\sum f_i A_i} \quad (2.13)$$

Here A_{comp} is the total atomic weight of the elements in the compound [18, 33].

The detector system including 10 cm diameter NaI(Tl) detector by ORTEC Inc., connected to a multichannel pulse height analyzer are used. The sample was placed between the ^{152}Eu source and the detector. The measurements have been carried out in the range from 244 to 1528 keV. The measured photon attenuation coefficients μ , HVL , TVL were compared with the calculations obtained by using XCom [19].

The mass attenuation coefficient, μ_m (cm^2/g) for four different types of steel, calculated using the WinXCom code which uses chemical parameters of a mixture materials providing total cross sections as well as partial cross sections for various interaction processes at photon energy of 1 keV-1 GeV. The computation of the mass attenuation coefficients of the above five sample materials has been carried out by the mixture rule by using the WinXcom software for the mentioned energy range to present a comparison between the calculated and X-com values.

In this study, a Windows-based application software named EpiXS 2021 (available at <https://www.pnri.dost.gov.ph/index.php/downloads/software/epixs>) was used to calculate Z_{eff} and effective electron number. The software performs data library interpolation from 1 keV to 100 GeV and calculates partial or total cross sections (σ), mass attenuation coefficients (μ/ρ), linear attenuation coefficients (μ), mean free paths (mfp), HVL, Z_{eff} , and N_{eff} calculates [18].

3. RESULTS AND DISCUSSION

For two different steels, the μ/ρ have been calculated at photon energies of 1 keV-1 GeV and experimental measurement results were compared for the photon energies from 122 keV to 1408 keV. agreement for the present steels. It was observed that the experimental results and the theoretical calculation results were in good agreement.

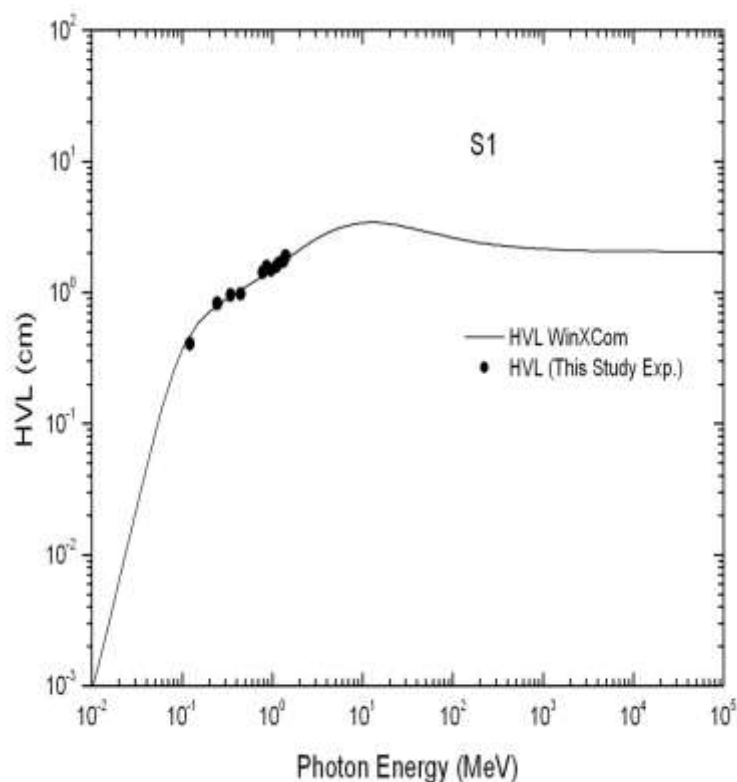


Fig 1. Experimental and calculated HVL for S1: EN 10204 and comparison with the experimental values (filled circle data).

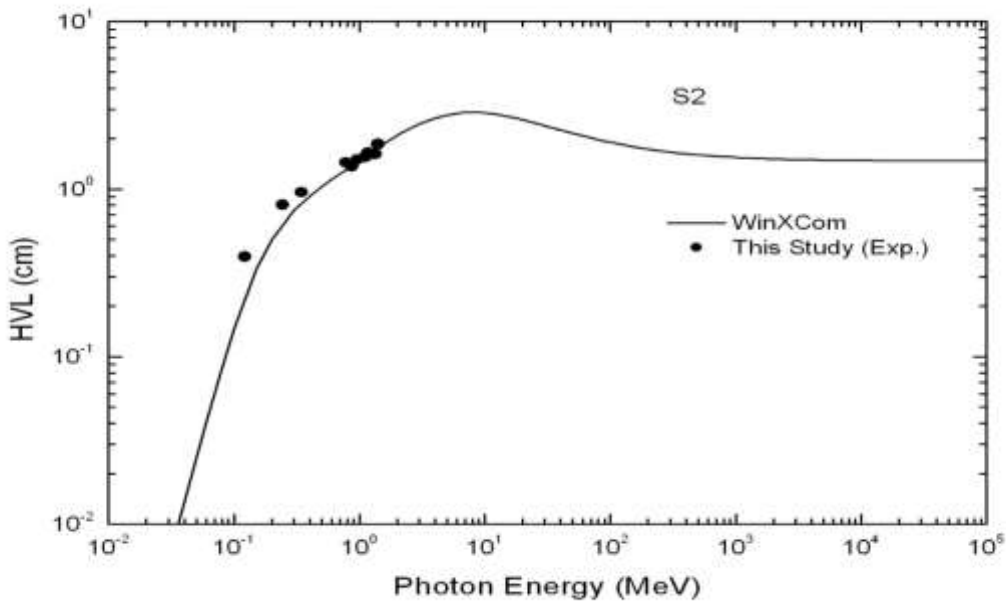


Fig 2. Experimental and calculated HVL for S2: EN 2367 and comparison with the experimental values (filled circle data).

The Z_{eff} for concretes at photon energies of 1 keV–100 GeV have been calculated using EpiXS 2021 code and the results were displayed in Figure 3 and 4 as a function of photon energy. This could be the result of different interaction processes of photon with the material for different energy ranges. The dominating photon interaction process is photoelectric absorption at low energies, Compton scattering (mainly incoherent) at intermediate energies, and pair production gradually becomes the dominant interaction process above about 1 MeV. Almost a constant structure has been observed after this energy.

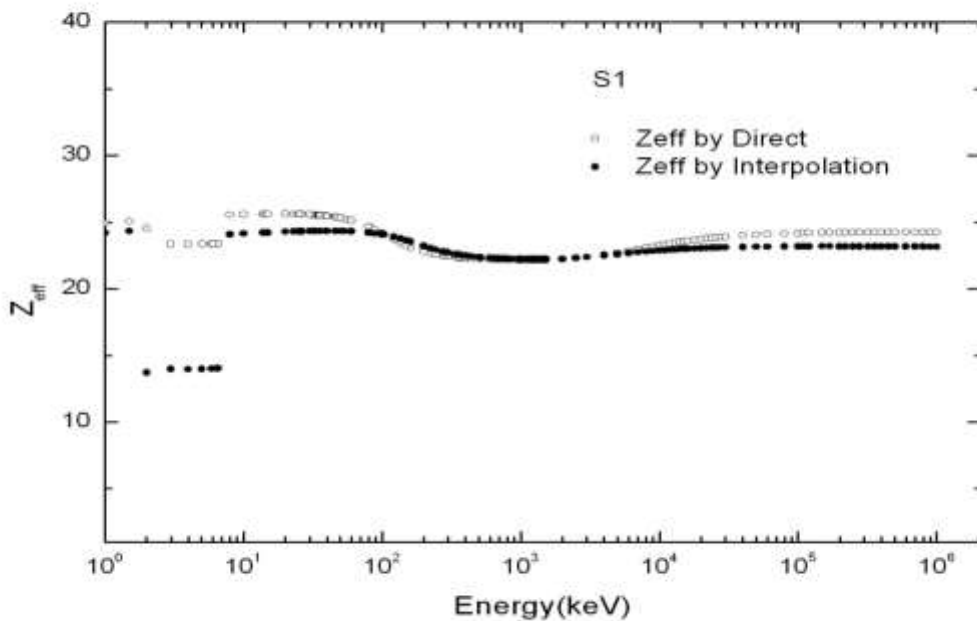


Figure 3 The Z_{eff} of concretes as a function of photon energy, for S1 samples respectively.

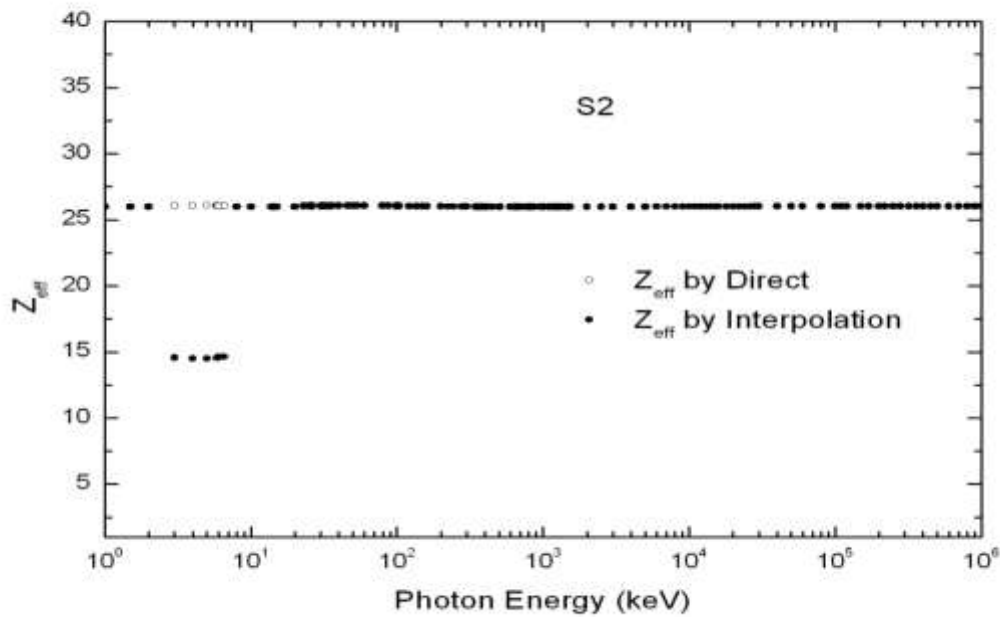


Figure 4 The Z_{eff} of concretes as a function of photon energy, for S2 samples respectively.

The effective electron numbers (N_{eff}) for concretes at photon energies of 1 keV-1 GeV have been calculated using EpiXS 2021 code and the results were displayed in Figure 5 and 6 as a function of photon energy. The results found directly and by interpolation are also shown in these figures. The values of N_{eff} found directly and by interpolation are between 100 keV and 7 MeV, while giving the same values, it differs below 100 keV and above 7 MeV.

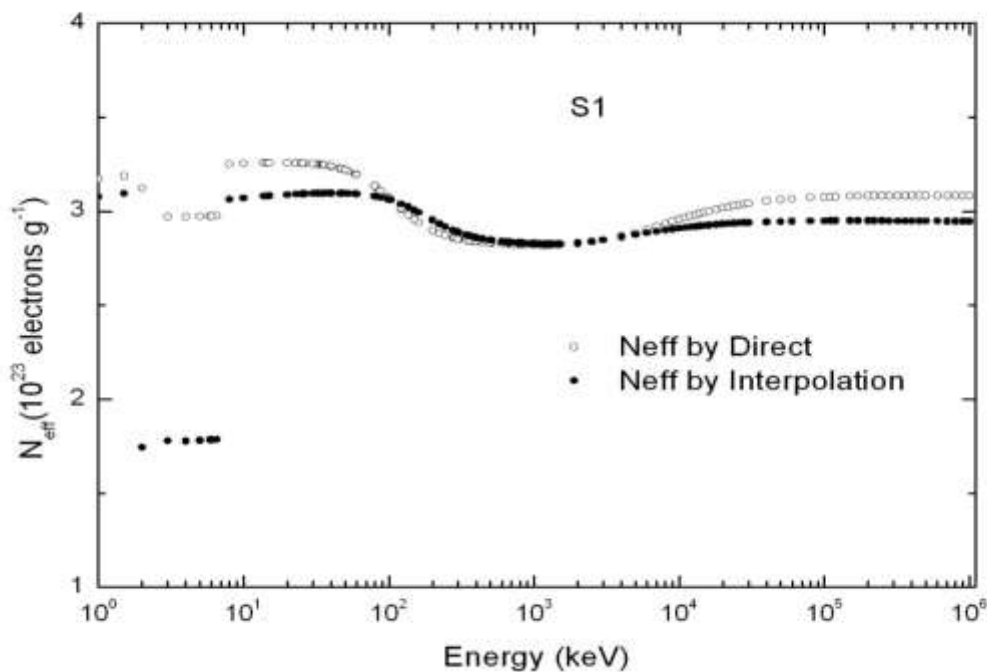


Figure 5. The N_{eff} of concretes as a function of incoming photon energy, for S1 and S2 samples respectively.

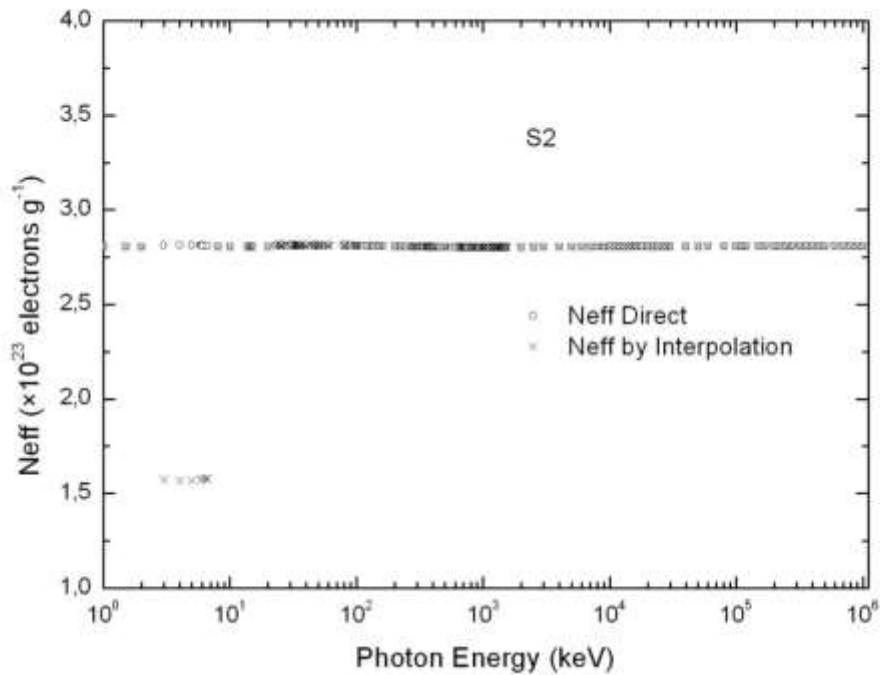


Figure 6. The N_{eff} of concretes as a function of incoming photon energy, for S1 and S2 samples respectively.

The Z_{eff} varies around 25 for S1 likewise, the N_{eff} varies around 3 for S1. However, for the S2 sample, both the Z_{eff} and the N_{eff} are almost constant.

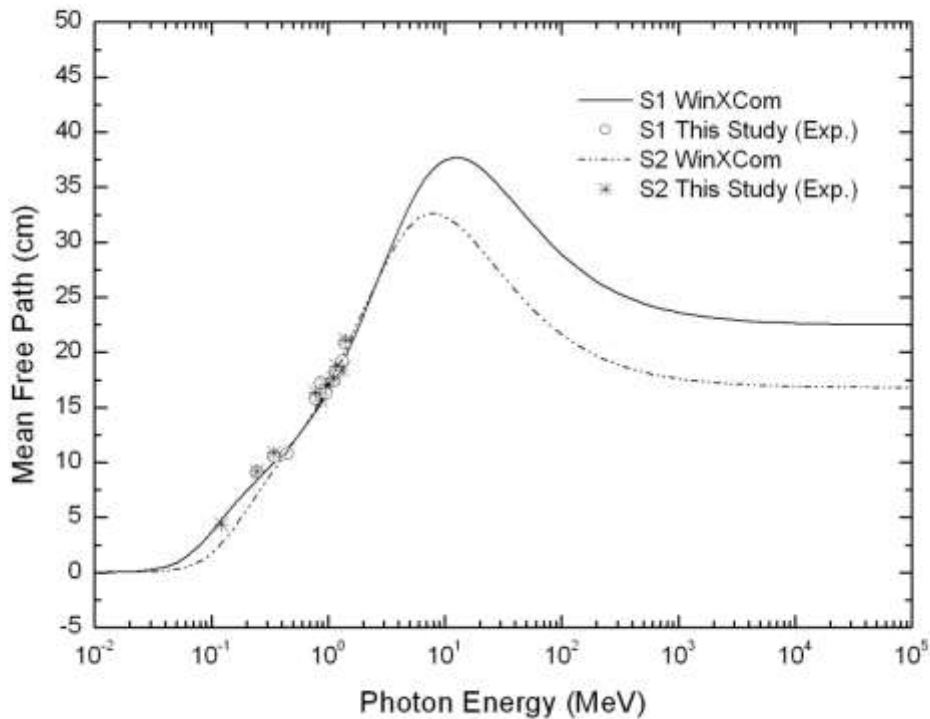


Figure 7. The mean free path of concretes as a function of incoming photon energy,

The photon mean free paths (λ) for concretes at the photon energies of 122, 245, 344, 444, 779, 867, 964, 1112, 1408, 1173 and 1333 keV have been calculated by using linear attenuation coefficients obtained from the measurements and the results were displayed in Figure 7 as a function of photon energy. It can be seen from this figure that the λ increased with the photon energy. As can be seen from Figure 9, the λ values calculated using WinXCom for samples S1 and S2 shows good agreement with the experimentally found values. It is very close to each other for the S1 and S2 samples in the energy region of interest. But, at energies above 3 MeV, the results obtained for S1 and S2 differ from each other.

4. CONCLUSION

According to the results obtained in this study, effective atom and electron numbers depend on the incident photon energies and the ratios of the materials in the compound. Half value layer (HVL) and the λ of concretes containing stainless steel (S1: EN 10204) and speed steel (S2: 2367). Z_{eff} and N_{eff} have been also calculated theoretically. In the interaction of photon with matter, the values of these parameters are dependent on the physical and chemical environments of the sample. The obtained mass attenuation coefficient values decrease with increasing photon energy. It was found that the experimental results of this work are in good agreement with the computed values. It could be concluded that the experimental results were consistent with the theoretical data. The results of this study will be helpful to understand better how mass attenuation coefficient values change with the variation in effective atomic numbers and effective electron densities of concretes.

ACKNOWLEDGMENTS

The authors would like to acknowledge Hascometal San. ve Tic. A.Ş and Osmanlı Alaşımli Çelikler San ve Tic. and to Kardemir A.Ş. for providing samples.

REFERENCES

- 1) Araz, S.O., Gümüő H., Bayca, S.U., Aydın, A., 2021. Appl Radiat Isot. Aydın Investigation of gamma-ray attenuation coefficients for solid boronized 304L stainless steel, 170, 1-7, <https://doi.org/10.1016/j.apradiso.2021.109605>
- 2) Lopez, G.E.P., Madrid, J.F., Abad, L.V., 2020. Chromium and cadmium adsorption on radiation-grafted polypropylene copolymers: regeneration, kinetics, and continuous fixed bed column studies. SN Applied Sciences 2 (3). <https://doi.org/10.1007/s42452-020-2168-7>
- 3) Bourland, J.D., 2016. Radiation oncology physics. In: Clinical Radiation Oncology. Elsevier, pp. 93–147. <https://doi.org/10.1016/b978-0-323-24098-7.00006-x>.
- 4) Manohara, S.R., Hanagodimath, S.M., 2007. Studies on effective atomic numbers and electron densities of essential amino acids in the energy range 1keV–100GeV. Nucl. Instrum. Methods Phys. Res. Sect. B Beam Interact. Mater. Atoms 258 (2), 321–328. <https://doi.org/10.1016/j.nimb.2007.02.101>.
- 5) Un, A., Caner, T., 2014. The Direct-Zeff software for direct calculation of mass attenuation coefficient, effective atomic number and effective electron number. Ann. Nucl. Energy 65, 158–165. <https://doi.org/10.1016/j.anucene.2013.10.041>
- 6) Singh, V.P., Medhat, M.E., and Shirmardi, S.P., 2015. Comparative studies on shielding properties of some steel alloys using Geant4, MCNP, WinXCOM and experimental results. *Radiation Physics and Chemistry*, 106,255-260.
- 7) Alim, B., Şakar, E., Baltakesmez, A., Han, İ., Sayyed, M.I., and Demir L. 2019. Experimental investigation of radiation shielding performances of some important AISI-coded stainless steels: Part I. *Radiation Physics and Chemistry*, 160, 108455. <https://doi.org/10.1016/j.radphyschem.2019.108455>.

- 8) Aygün, B., Akar E.S., Korkut, T., Sayyed, M.I., Karabulut, A., Zaid, M.H.M., 2019. Fabrication of Ni, Cr, W reinforced new high alloyed stainless steels for radiation shielding applications, *Results Phys* 12, 1-6. <https://doi.org/10.1016/j.rinp.2018.11.038>.
- 9) Abbasova, N., Yüksel, Z., Abbasov, E., Gülbiçim, H., Tufan, M.Ç., 2019. Investigation of gamma-ray attenuation parameters of some materials used in dental applications. *Results in Physics* 12, 2202–2205. <https://doi.org/10.1016/j.rinp.2019.02.068>.
- 10) Singh, V.P., Badiger, N.M., 2013. Study of mass attenuation coefficients, effective atomic numbers and electron densities of carbon steel and stainless steels, *Radioprotection* 48, 431e443, <https://doi.org/10.1051/radiopro/2013067>.
- 11) Singh, V.P., Badiger, N.M., The gamma-ray and neutron shielding factors of fly-ash brick materials, *Radiological Protection*, 34, 89-101, 2014.
- 12) Pogribny, I.P., 2017. Environmental exposures and epigenetic perturbations. In: *Reference Module in Biomedical Sciences*. Elsevier. <https://doi.org/10.1016/b978-0-12-801238-3.65062-6>.
- 13) El-Khayatt, A. M., Ali A. M., Vishwanath P. Singh, Badiger, N., 2014. Determination of mass attenuation coefficient of low-Z dosimetric materials, *Radiat. Eff. and Deff. In Solids*, 169, 12, 1038-1044.
- 14) Berger, M., Hubbell, J., Seltzer, S., Chang, J., Coursey, J., Sukumar, R., Zucker, D., Olsen, K., 2010. XCOM: Photon Cross Sections Database. NIST standard reference database 8 (XGAM). <https://doi.org/10.18434/T48G6X>.
- 15) Berger, M.J., Hubbell, J.H., 1987. NBSIR 87-3597, XCOM: Photon Cross Sections on a Personal Computr. National Institute of Standards, Gaithersburg, MD 20899, USA. <http://physics.nist.gov/PhysRefData/Xcom/Text/XCOM.html>.
- 16) Berger, M., Hubbell, J., Seltzer, S., Chang, J., Coursey, J., Sukumar, R., Zucker, D., Olsen, K., 2004. Tables of X-Ray Mass Attenuation Coefficients and Mass Energy-Absorption Coefficients from 1 keV to 20 MeV for Elements Z=1 to 92 and 48 Additional Substances of Dosimetric Interest. NIST standard reference database 126 (XGAM). <https://doi.org/10.18434/T4D01F>.
- 17) Hila, F.C., Amorsolo Jr., A.V., Javier-Hila, A.M.V., Guillermo, N.R.D., 2020. A simple spreadsheet program for calculating mass attenuation coefficients and shielding parameters based on EPICS2017 and EPDL97 photoatomic libraries. *Radiat. Phys. Chem.* 177, 109122. <https://doi.org/10.1016/j.radphyschem.2020.109122>.
- 18) Hila, F.C., Asuncion-Astronomo, A., Dingle, C.A.M., Jecong, J.F.M., Javier-Hila, A.M.V., Gili, M.B.Z., Balderas, C.V., Lopez, G.E.P., Guillermo, N.R.D., Amorsolo, A.V., Jr., 2021. EpiXS: A Windows-based program for photon attenuation, dosimetry and shielding based on EPICS2017 (ENDF/B-VIII) and EPDL97 (ENDF/B-VI.8). *Radiation Physics and Chemistry*, 109331.
- 19) Gerward, L., Guilbert, N., Jensen, K.B., Levring, H., 2004. WinXCom-a program for calculating X-ray attenuation coefficients. *Radiat. Phys. Chem.* 71 (3–4), 653–654. <https://doi.org/10.1016/j.radphyschem.2004.04.040>
- 20) Büyük, B., Tuğrul, A.B., 2014. An investigation on gamma attenuation behaviour of titanium diboride reinforced boron carbide–silicon carbide composites, *Radiation Physics and Chemistry* 97, 354-359. <https://doi.org/10.1016/j.radphyschem.2013.07.025>
- 21) Elmahroug, Y., Tellili, B., Souga, C., Manai, K., 2015. ParShield: a computer program for calculating attenuation parameters of the gamma rays and the fast neutrons. *Ann. Nucl. Energy* 76, 94-99. <https://doi.org/10.1016/j.anucene.2014.09.044>.

- 22) Ađar O., Tekin H.O., Sayyed M.I., Korkmaz M.E., Culfa O., Ertugay C., 2019. Experimental investigation of photon attenuation behaviors for concretes including natural perlite mineral, *Results Phys* 12, 237-243, <https://doi.org/10.1016/j.rinp.2018.11.053>.
- 23) Hubbell, J.H., 1982. Photon mass attenuation and energy-absorption coefficients, *Int. J. Appl. Radiat. Isot.* 1982. [https://doi.org/10.1016/0020-708X\(82\)90248-4](https://doi.org/10.1016/0020-708X(82)90248-4).
- 24) Hubbell JH, Seltzer SM. 1995. Tables of X-ray mass attenuation coefficients and mass energy absorption coefficients 1 keV to 20 MeV for elements Z=1 to 92 and 48 additional substances of dosimetric interest, in, National Inst. of Standards and Technology-PL, Gaithersburg, MD (United States). Ionizing Radiation Div.; 1995
- 25) Akman F., Kađal M.R., Akman F., Soyulu M.S., 2017. Determination of effective atomic numbers and electron densities from mass attenuation coefficients for some selected complexes containing lanthanides, *Can. J. Phys.* 95 (10), 1005-1011. <https://doi.org/10.1139/cjp-2016-0811>.
- 26) Akman, F., Kađal, M.R., Sayyed, M.I., Karatas, H.A., 2019. Study of gamma radiation attenuation properties of some selected ternary alloys. *J. Alloys Compd.* 782, 315–322. <https://doi.org/10.1016/j.jallcom.2018.12.221>.
- 27) Sayyed, M.I., Kaky, K.M., S,akar, E., Akbaba, U., Taki, M.M., Agar, O., 2019. Gamma radiation shielding investigations for selected germanate glasses. *J. Non-Cryst. Solids* 512, 33–40. <https://doi.org/10.1016/j.jnoncrysol.2019.02.014>.
- 28) Sayyed, M.I., Mahmoud, K.A., Islam, S., Tashlykov, O.L., Lacomme, E., Kaky, K.M., 2020. Application of the MCNP 5 code to simulate the shielding features of concrete samples with different aggregates. *Radiat. Phys. Chem.* 174, 108925 <https://doi.org/10.1016/j.radphyschem.2020.108925>.
- 29) Gowda S, Krishnaveni S, Yashoda T, Umesh TK, Gowda R., 2004. Photon mass attenuation coefficients, effective atomic numbers and electron densities of some thermoluminescent dosimetric compounds. *Prama-J. Phys.* 63, 529-41.
- 30) Han I, Demir L. 2009. Mass attenuation coefficients, effective atomic and electron numbers of Ti and Ni alloys. *Radiat Meas*, 44, 289–94.
- 31) Singh, T., Kaur, P., Singh, P.S., 2007. A study of photon interaction parameters in some commonly used solvents. *J. Radiol. Prot.* 27 (1), 79–85. <https://doi.org/10.1088/0952-4746/27/1/005>.
- 32) Taylor, M.L., Smith, R.L., Dossing, F., Franich, R.D., 2012. Robust calculation of effective atomic numbers: the Auto-Zeffsoftware. *Med. Phys.* 39 (4), 1769–1778. <https://doi.org/10.1118/1.3689810>.
- 33) Prabhu, S., Sneha, A.C., Shetty, P.P., Narkar, A.A., Bubbly, S.G., Gudennavar, S.B., 2020. Effective atomic number and electron density of some biologically important lipids for electron, proton, alpha particle and photon interactions. *Appl. Radiat. Isot.* 160, 109137 <https://doi.org/10.1016/j.apradiso.2020.109137>.